JCTC Journal of Chemical Theory and Computation

ARTICLE

pubs.acs.org/JCTC

Edge Stabilities of Hexagonal Boron Nitride Nanoribbons: A First-Principles Study

Rajdip Mukherjee*,† and Somnath Bhowmick*,‡

†Department of Materials Engineering, Indian Institute of Science, Bangalore, India

‡Materials Research Center, Indian Institute of Science, Bangalore, India

ABSTRACT: We investigate the comparative stability of sp^2 bonded planar hexagonal boron nitride (h-BN) nanoribbon (BNNR) edges, using first principles calculations. We find that the pristine armchair edges have the highest degree of stability. Pristine zigzag edges are metastable, favoring planar reconstructions [in the form of 5−7 rings] that minimizes the energy. Our investigation further reveals that the pristine zigzag edges can be stabilized against 5−7 reconstructions by passivating the dangling bonds at the edges by other elements, such as hydrogen (H) atoms. Electronic and magnetic properties of nanoribbons depend on the edge shapes and are strongly affected by edge reconstructions.

1. INTRODUCTION

The area of research on two-dimensional material has seen tremendous growth in the past few years, driven by fundamental physics as well as potential next generation device applications. Although graphene has been the frontrunner until now,[1,2] single layer hexagonal boron nitride (h-BN) and it's hybrids with graphene have drawn a great deal of attention of late.[3−6]

Similar to graphene,[7,8] single (or a few) layers of h-BN sheets have been prepared using micromechanical cleaving and chemically derived routes.[9,10] One-dimensional nanoribbons of graphene[11] and h-BN[12] have also been successfully synthesized. Due to novel electronic and magnetic properties,[1,2,13−16] nanoribbons are of great interest. On the basis of the shape, edges of nanoribbons can be classified as zigzag and armchair, as shown in Figure 1a and b, respectively. Electronic and magnetic properties of the nanoribbons depend on edge shapes.[1,4,5] Thus, determining the stability of different edges is crucial for the purpose of technological applications of nanoribbons in future generation devices.

Structural instabilities at the edges and resulting reconstructions are well-known in graphene nanoribbons.[17−22] Certain reconstructions are found to induce compressive stress along the edge, which is released by warping of the nanoribbon.[22] The stability of various different edges of graphene nanoribbons can be controlled by experimental conditions and depend on the nature of edge passivation.[19] As reported by Koskinen et al.,[18] edge reconstructions are also self-passivating for metastable unpassivated zigzag graphene nanoribbons and lower the edge energy. Surprisingly, the stability of BNNR edges has hardly been discussed in the literature. Although Ding et al.[23] have studied the pristine BNNR edges as a function of H-passivation, to the best of our knowledge, the possibility of self-passivating edge reconstructions in h-BN nanoribbons remains unexplored.

In this work, we report a comparative study of the stability of different edges of h-BN nanoribbons. Other than the regular pristine armchair and zigzag edge, we also consider a reconstructed edge, made of 5−7 rings. Such reconstructions create homoelemental B−B and N−N bonds [see Figure 1c], which are higher in energy than the B−N bonds and thus unfavorable.[24] Hence, unlike graphene nanoribbons (see previous paragraph), 5−7 reconstructions are not guaranteed to lower the edge formation energy of unpassivated zigzag BNNR, and we investigate whether they can be self-passivating in the latter. Other than the self-passivating reconstructions, nanoribbon edges can also be stabilized by saturating the dangling bonds with other elements, such as H atoms.[19] Our study also reveals how H-passivation affects the stability of various different BNNR edges: pristine and 5−7 reconstructed.

This paper is organized as follows. We describe computational details in section 2. The main findings of our work are reported in section 3. First, we discuss the edge stability of nanoribbons: unpassivated BNNRs in section 3.1 and H-passivated BNNRs in section 3.2. We present a comparison between graphene and h-BN nanoribbons in section 3.3. Keeping in mind the importance of the electronic and magnetic properties of nanoribbons, we briefly describe how they are affected by the edge reconstructions in section 3.4. The paper is concluded in section 4.

2. METHOD

We use first-principles calculations as implemented in the PWSCF code,[25] with a plane-wave basis set and ultrasoft pseudopotential, and the electron exchange-correlation is treated within a generalized gradient approximation (GGA), as described by Perdew et al.[26] We use an energy cutoff for the plane-wave basis for wave functions (charge density) of 40 (400) Ry. Nanoribbons are simulated using a supercell geometry, with a vacuum layer of ∼15 Å between any two periodic images of the BNNR. A k-point grid of $1 \times 12 \times 1$ k points (periodic direction of the ribbon along the y axis) is used for sampling Brillouin zone integrations. The length of periodicity L [$3a$, $(3a)^{1/2}$, and $2 \times (3a)^{1/2}$ for pristine armchair, pristine zigzag, and edge reconstructed zigzag, respectively] is fixed according to the equilibrium lattice parameter of h-BN (a = 1.45 Å). We allow the structure to fully relax

Received: November 6, 2010
Published: January 10, 2011

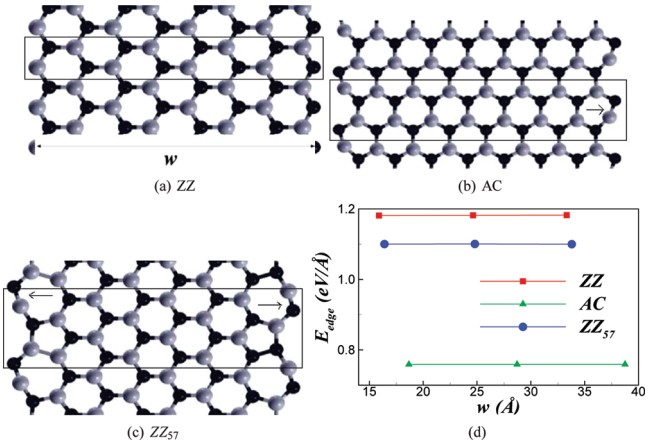

Figure 1. Unpassivated (a) pristine ZZ and (b) pristine AC h-BN nanoribbon of width w. The ribbons are periodic in the direction perpendicular to w. The rectangular box represents the repeat unit of each nanoribbon. N (B) atoms are shown in black (gray). Arrows mark the triple bonds (length ∼ 1.3 Å). (c) Edge reconstructed zigzag h-BN nanoribbon—ZZ_{57}; 5−7 defects create homoelemental B−B and N−N bonds. (d) Edge formation energy [see eq 1 and Table 1] as a function of w; E_{edge} does not depend on ribbon width. Pristine AC nanoribbon has the lowest edge formation energy, followed by ZZ_{57} and pristine ZZ.

until the force on every atom is less than 10^{-3} Ry/au and total energy changes are smaller than 10^{-4} Ry.

We analyze the stability of edges by comparing the edge formation energy per unit length, defined as

$$E_{edge} = \frac{1}{2L}\left[E_{tot} - N_{BN}E_{BN} - \frac{N_H}{2}E_{H_2}\right] \quad (1)$$

where E_{tot}, E_{BN}, and E_{H_2} are the total energy of the nanoribbon supercell, the energy of a BN pair in bulk h-BN, and the energy of the H_2 molecule; N_{BN} (N_H) is the number of BN pairs (H atoms) in the nanoribbon [$N_H = 0$ for the unpassivated BNNRs]. L is the periodic length along the ribbon axis, and the factor 2 in the denominator accounts for the two edges present per repeated unit. Since BNNRs have asymmetric edges [other than the armchair nanoribbon; for example, compare Figure 1a and b], periodic boundary condition gives rise to an artificial electric field across the width of the ribbon. Dipole correction, as implemented in the PWSCF code,[27] is employed to cancel this artificial field and calculate the correct total energy of the ribbon, E_{tot}. Stress along the edge or periodic direction is reported as $\sigma = V\sigma_{yy}/L$, where σ_{yy} is the diagonal element of the stress tensor in the y direction (defined along the ribbon axis) and V is the volume of the supercell. We use +ve and −ve σ to denote compressive and tensile stress, respectively. σ_{yy} is calculated using the Nielsen−Martin algorithm,[28] as implemented in the PWSCF code.

3. RESULTS AND DISCUSSIONS

3.1. Unpassivated BNNRs. The relaxed structures of unpassivated pristine zigzag (ZZ), pristine armchair (AC), and edge-reconstructed zigzag (ZZ_{57}) ribbons are shown in Figure 1a,b,c, respectively. The subscript 57 indicates that the edge reconstructions take place via the formation of 5−7 rings or Stone−Wales (SW) defects.[29] Such topological defects form in a honeycomb lattice by 90° rotation of B−N (C−C) bonds in h-BN[30] (graphene[31]) and are relevant for their mechanical behavior.

Table 1. Edge Formation Energy and Stress (Along the Ribbon Edge) of h-BN Nanoribbons[a]

ribbon	w (Å)	E_{edge} (eV/Å)	σ (eV/Å)
ZZ	15.89	1.1813	0.30
	24.63	1.1819	0.30
	33.33	1.1825	0.32
AC	18.67	0.7587	0.25
	28.72	0.7588	0.26
	38.75	0.7590	0.27
ZZ_{57}	16.40	1.1003	−4.97
	24.80	1.1006	−5.07
	33.80	1.1008	−5.08
ZZ^H	18.15	0.1217	−0.21
	26.85	0.1218	−0.22
	35.54	0.1218	−0.22
AC^H	20.77	0.1164	−0.19
	30.84	0.1172	−0.20
	40.86	0.1177	−0.20
ZZ_{57}^H	18.70	0.6400	−3.70
	27.43	0.6405	−3.76
	36.16	0.6401	−3.85
$ZZ_{5'7'}^H$	18.67	0.9309	−2.55
	27.37	0.9321	−2.57
	36.07	0.9327	−2.67

[a] See eq 1 and text thereafter for the definition of E_{edge} and σ.

As mentioned previously, SW defects create energetically unfavorable homoelemental (B−B and N−N) bonds in h-BN[24] [see Figure 1c]. The edge formation energies, calculated using eq 1, are plotted in Figure 1d and reported in Table 1. E_{edge} (as well as σ) hardly changes as the ribbon width increases by a factor of 2. This gives us confidence that the numerical values reported here for those two parameters are indeed well converged.

We find that pristine armchair BNNR has lower edge formation energy than that of pristine zigzag. Similar to bare edge graphene nanoribbons,[18,19] triple bonds are formed at the armrests [shown by the arrow in Figure 1b], which is evident from their bond length of 1.30 Å, 10% shorter than the sp^2 bonds of the two-dimensional h-BN. Zigzag BNNR cannot form triple bonds and have a higher formation energy due to the existence of expensive dangling bonds at the edges. As shown in Figure 1c, triple bonding (length 1.30 Å) is also observed in ZZ_{57}, which lowers the edge formation energy by 0.08 eV/Å, compared to that of pristine zigzag BNNR. Thus, we conclude that *the gain due to triple bond formation (which eliminates the dangling bonds at the edges) is more than the energy expense of unfavorable homoelemental bond creation*, making ZZ_{57} relatively favorable than the pristine ZZ BNNR. However, AC is the most stable of the BNNRs, its edge formation energy being 30% smaller than that of ZZ_{57}.

As reported in Table 1, pristine BNNRs are under little compressive stress. It is well-known that compressive stress is relieved by wrinkle formation in graphene nanoribbons.[22,32] However, we have found that the stress is too small to show any significant out of plane deformation in pristine BNNRs. On the other hand, 5−7 reconstructions induce great tensile stress along the ribbon edge, which ensures the planarity of such BNNRs.

3.2. H-Passivated BNNRs. Nanoribbon edges can be stabilized by saturating the dangling bonds with H atoms (or any other molecule in general). Note that there is no further scope of

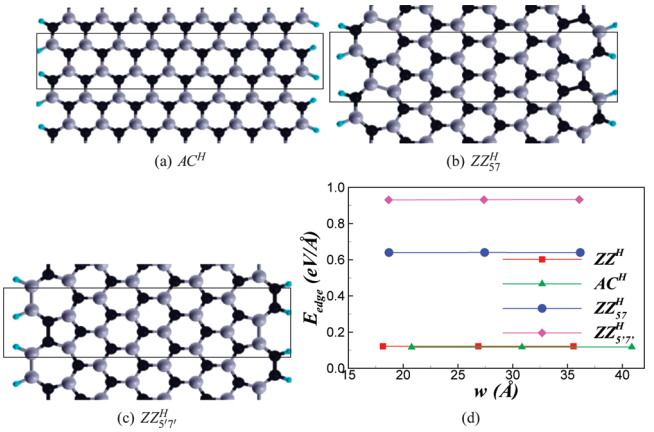

Figure 2. (a) Hydrogen passivated pristine AC^H h-BN nanoribbon. Note that H termination leads to smoother edges [compare with Figure 1b]. The shape of the pristine ZZ^H h-BN nanoribbon is very similar to that in Figure 1a. Two types of reconstructions, ZZ^H_{57} and $ZZ^H_{5'7'}$, are shown in b and c, respectively. The latter has twice the number of homoelemental B−B and N−N bonds per repeat unit than the former. (d) Edge formation energy [see eq 1 and Table 1] as a function of ribbon width w; E_{edge} does not depend on ribbon width. H passivation stabilizes the pristine zigzag BNNR, edge formation energy being nearly equal to that of the pristine armchair BNNR, and reconstructions are unfavorable.

triple bonding for the edge atoms (of both armchair and zigzag nanoribbons), as they form sp^2 bonds with two neighboring B (or N) atoms and a H atom each. This eliminates the difference in the nature of chemical bonding of pristine zigzag and armchair edge atoms (explained in the previous section for unpassivated BNNRs), which is manifested in respective edge formation energies, being nearly equal in ZZ^H and AC^H [see Figure 2d and Table 1]. The superscript H is used to mark the hydrogen-terminated BNNRs.

We observe that H termination reduces the edge formation energy and changes σ to small tensile stress in pristine BNNRs [see Table 1]. Comparing Figure 2a and Figure 1b, it is clear that H termination makes the equilibrium shape of the armchair BNNR edges smoother. Bare and H-passivated pristine zigzag BNNR have a similar equilibrium edge shape, and we do not illustrate the structure of the latter in the paper. We study two types of edge reconstructions in H-passivated zigzag BNNR, ZZ^H_{57} and $ZZ^H_{5'7'}$, as shown in Figure 2b and c. Both the reconstructions induce tensile stress along the ribbon edge [see Table 1], and the resulting nanoribbons have planar geometry. We have verified that the $5'-7'$ reconstruction is not stable in unpassivated BNNR. Though both are made of 5−7 rings, $ZZ^H_{5'7'}$ has a higher E_{edge}, albeit having a smaller σ (costing lesser strain energy) than that of ZZ^H_{57} [consult Figure 2d and Table 1]. Higher edge formation energy can be attributed to the higher linear density of unfavorable B−B and N−N bonds in the former [see Figure 2b and c; $ZZ^H_{5'7'}$ has double the number of homoelemental bonds per repeat unit than ZZ^H_{57}]. Comparing the values of E_{edge} [Figure 2d and Table 1], we conclude that unlike the bare zigzag BNNR, edge reconstructions are not favorable in H-terminated zigzag BNNR; 5−7 ($5'-7'$) reconstruction increases the edge formation energy by ∼5.5 (8) times. Thus, *edge passivation offers a simple way to stabilize the pristine zigzag edge against* 5−7 *reconstructions in BNNRs.*

3.3. Comparison with Graphene Nanoribbons. Graphene and h-BN have several similarities. Not only do they have

Table 2. Magnetic Property and Band Gap (E_g) of the BNNRs Shown in Figure *1* and *2*

BNNR	magnetic property	E_g (eV)
ZZ	magnetic	metallic
AC	nonmagnetic	4.8
ZZ_{57}	nonmagnetic	2.7
ZZ^H	nonmagnetic	5.0
AC^H	nonmagnetic	5.5
ZZ^H_{57}	nonmagnetic	2.6
$ZZ^H_{5'7'}$	nonmagnetic	1.7

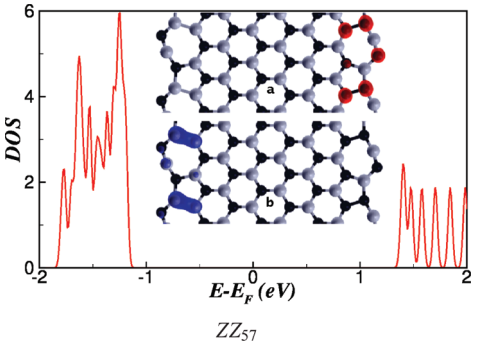

Figure 3. Unpassivated, edge reconstructed BNNR densities of state (DOS) and band decomposed electron densities of (a) the top of the valence band and (b) the bottom of the conduction band, localized mainly at the N−N and B−B bonds, created by 5−7 defects. We have used XCRYSDEN[35] to plot the charge densities.

identical structures (constituent atoms are arranged in a honeycomb lattice) but also their values of cohesive energy (in-plane stiffness) are within ∼5 (∼18%) of each other.[33] Thus, it is worth comparing the edge formation energies and reconstructions of graphene and h-BN nanoribbons.

In the case of unsaturated nanoribbons, we observe two major differences. First, the 5−7 reconstructed edge has the lowest formation energy, followed by the pristine armchair edge in graphene nanoribbons.[18,19] As shown here, the sequence happens to be opposite in unpassivated BNNRs. Second, self-passivating 5−7 reconstruction in bare zigzag graphene is more effective than that in the bare zigzag h-BN nanoribbon. While E_{edge} of the reconstructed zigzag graphene nanoribbon is ∼17%[18,19] smaller than that of the bare pristine zigzag graphene nanoribbon, we find that similar edge reconstruction leads to an energy gain of ∼6% [see Table 1] in the unpassivated zigzag h-BN nanoribbon. Such distinctions can be understood from the formation energy of the SW defect in graphene and h-BN: ∼5 eV[31] and ∼6−6.5 eV,[34] respectively. As mentioned previously, higher formation energy in the latter is due to energetically unfavorable B−B and N−N bonds, created by the SW defect in h-BN.[24]

Due to a similar reason, between the H-saturated zigzag BNNR and graphene, edge reconstructions are more unfavorable in the former. Comparing the edge formation energies, we find that 5−7 reconstructions augment E_{edge} by −450% to 700% in H-terminated zigzag BNNR [see Table 1], larger than a 300% increase in the H-passivated zigzag graphene nanoribbon.[19] Since pristine BNNRs are devoid of homoelemental bonds, they show similar behavior to graphene nanoribbons on H passivation, which reduces the edge formation energy by ∼90% in both

dx.doi.org/10.1021/ct1006345 |J. Chem. Theory Comput. 2011, 7, 720–724

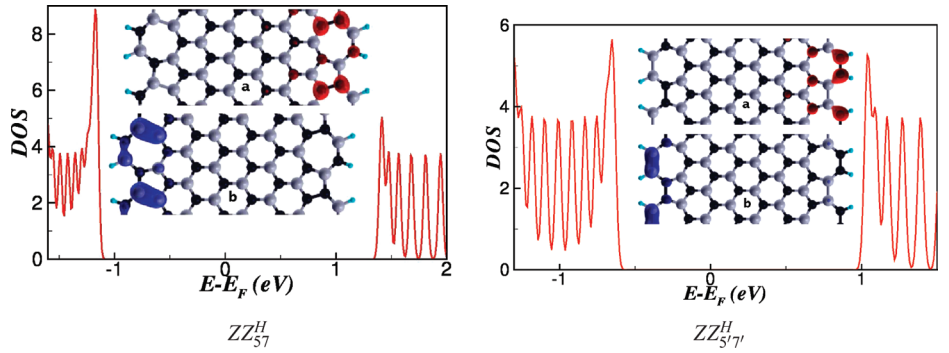

ZZ^{H}_{57} $ZZ^{H}_{5'7'}$

Figure 4. H-passivated, edge-reconstructed BNNR densities of state (DOS) and band decomposed electron densities. In the inset, we show charge density of (a) the top of the valence band and (b) the bottom of the conduction band, localized mainly at the N−N and B−B bonds, created by 5−7 defects. This appears to be a general phenomenon associated with 5−7 defects and also observed in unpassivated BNNRs [see Figure 3].

the systems [compare the values reported in Table 1 and by Wassmann et al.[19]].

3.4. Electronic and Magnetic Properties. Finally, we briefly discuss the electronic and magnetic properties of BNNRs, summarized in Table 2. Other than the unpassivated pristine zigzag, all of the BNNRs are nonmagnetic and have band gaps ranging from 1.7 to 5.5 eV. The magnetic moment originates from the dangling bonds at the edges. Our results are in good agreement with those of Barone and Peralta,[13] where the authors have discussed the electronic and magnetic properties of pristine BNNRs in great detail. In this paper, we rather restrict ourselves to the discussion of electronic and magnetic properties of edge-reconstructed BNNRs.

We find that 5−7 reconstruction is detrimental for the edge magnetic moment. In pristine unpassivated zigzag BNNR, the magnetic moment is found to be 1 Bohr magneton per edge atom, which vanishes completely in ZZ_{57}. Similar behavior has been observed in edge-reconstructed graphene nanoribbons.[17,22] We show the electronic densities of state (DOS) of ZZ_{57} BNNR in Figure 3 . While the pristine unpassivated zigzag BNNR is metallic, 5−7 defects open up a gap of 2.7 eV. The inset of Figure 3 illustrates the charge density of the top of the valence band and bottom of the conduction band. Interestingly, they are confined at N−N and B−B bonds, created by the 5−7 defects. Thus, such sites are expected to play a major role in electronic applications and the chemical reactivity of edge-reconstructed BNNRs. As shown in Figure 4, similar behavior is observed in H-passivated, edge-reconstructed BNNRs also. While pristine H-passivated BNNR has a band gap of 5.0 eV, 5−7 edge reconstructions reduces it by at least 50% or more.

4. SUMMARY AND CONCLUSIONS

We have investigated the edge stability and emerging electronic and magnetic properties of h-BN nanoribbons. In terms of dangling bond saturations, we divide BNNRs into two groups, unpassivated and H-passivated. Among unsaturated BNNRs, armchair edges are found to have minimum formation energy, followed by ZZ_{57}. In both of the ribbons, edge atoms form triple bonds, replacing the dangling bonds and minimizing the edge formation energy in the process. Atoms located at the bare zigzag edges cannot form triple bonds, and ZZ BNNR has the highest E_{edge} due to the presence of dangling bonds. However, 5−7 rings create energetically unfavorable homoelemental B−B and N−N bonds, and edge reconstructions of bare zigzag BNNRs are not as effective as they are in bare zigzag graphene nanoribbons. Saturating the dangling bonds at the edges by H not only minimizes the edge formation energies but also imparts stability to the pristine zigzag edge against 5−7 reconstructions.

Controlling the edge shape is important for the application of nanoribbons in devices because electronic and magnetic properties depend on the geometry of the edges. We find that 5−7 reconstructions destroy the edge magnetism observed in pristine unpassivated zigzag BNNR. In H-passivated ZZ BNNR, such reconstructions reduce the band gap. Our results show that, depending on edge shape, BNNRs can be magnetic or nonmagnetic and metallic or semiconducting, having a moderate to wide band gap. Such a rich collection of properties shows how promising h-BN nanoribbons are for application in future generation electronic devices.

Note added: After the completion of the paper, we came to know about a similar work[36] discussing the stability of pristine zigzag and armchair edges of h-BN sheets, and the results are in good agreement with our findings. However, the authors of the other paper did not consider edge reconstructions, which we discuss in great detail.

AUTHOR INFORMATION

Corresponding Author

*E-mail: rajdip@platinum.materials.iisc.ernet.in (R.M.); bsomnath@mrc.iisc.ernet.in (S.B.).

ACKNOWLEDGMENT

We thank SERC, IISc for providing computational facilities. S.B. thanks Umesh V. Waghmare for useful discussions on stability and reconstructions of nanoribbon edges.

REFERENCES

(1) Neto, A. H. C.; Guinea, F.; Peres, N. M. R.; Novoselov, K. S.; Geim, A. K. *Rev. Mod. Phys.* **2009**, *81*, 109.
(2) Geim, A. K.; Novoselov, K. S. *Nat. Mater.* **2007**, *6*, 183–191.
(3) Golberg, D.; Bando, Y.; Huang, Y.; Terao, T.; Mitome, M.; Tang, C.; Zhi, C. *ACS Nano* **2010**, *4*, 2979–2993.
(4) Blase, X.; Rubio, A.; Louie, S. G.; Cohen, M. L. *Phys. Rev. B* **1995**, *51*, 6868–6875.
(5) Park, C.-H.; Louie, S. G. *Nano Lett.* **2008**, *8*, 2200–2203. PMID: 18593205.
(6) Ci, L.; Song, L.; Jin, C.; Jariwala, D.; Wu, D.; Li, Y.; Srivastava, A.; Wang, Z. F.; Storr, K.; Balicas, L.; Liu, F.; Ajayan, P. M. *Nat. Mater.* **2010**, *9*, 430–435.

(7) Novoselov, K. S.; Jiang, D.; Schedin, F.; Booth, T. J.; Khotkevich, V. V.; Morozov, S. V.; Geim, A. K. *Proc. Natl. Acad. Sci. U.S.A.* **2005**, *102*, 10451–3.
(8) Rao, C. N. R.; Sood, A. K.; Subrahmanyam, K. S.; Govindaraj, A. *Angew. Chem.* **2009**, *48*, 7752–7777.
(9) Pacilé, D.; Meyer, J. C.; Girit, Ç. Ö.; Zettl, A. *Appl. Phys. Lett.* **2008**, *92*, 133107.
(10) Han, W.-Q.; Wu, L.; Zhu, Y.; Watanabe, K.; Taniguchi, T. *Appl. Phys. Lett.* **2008**, *93*, 223103.
(11) Han, M. Y.; Özyilmaz, B.; Zhang, Y.; Kim, P. *Phys. Rev. Lett.* **2007**, *98*, 206805.
(12) Chen, Z.-G.; Zou, J.; Liu, G.; Li, F.; Wang, Y.; Wang, L.; Yuan, X.-L.; Sekiguchi, T.; Cheng, H.-M.; Lu, G. Q. *ACS Nano* **2008**, *2*, 2183–2191.
(13) Barone, V.; Peralta, J. E. *Nano Lett.* **2008**, *8*, 2210–2214.
(14) Chen, W.; Li, Y.; Yu, G.; Li, C.-Z.; Zhang, S. B.; Zhou, Z.; Chen, Z. *J. Am. Chem. Soc.* **2010**, *132*, 1699–1705.
(15) Wu, X.-j.; Wu, M.-h.; Zeng, X. *Front. Phys. China* **2009**, *4*, 367–372.
(16) Yao, W.; Yang, S. A.; Niu, Q. *Phys. Rev. Lett.* **2009**, *102*, 096801.
(17) Huang, B.; Liu, M.; Su, N.; Wu, J.; Duan, W.; lin Gu, B.; Liu, F. *Phys. Rev. Lett.* **2009**, *102*, 166404.
(18) Koskinen, P.; Malola, S.; Häkkinen, H. *Phys. Rev. Lett.* **2008**, *101*, 115502.
(19) Wassmann, T.; Seitsonen, A. P.; Saitta, A. M.; Lazzeri, M.; Mauri, F. *Phys. Rev. Lett.* **2008**, *101*, 096402.
(20) Girit, C. O.; Meyer, J. C.; Erni, R.; Rossell, M. D.; Kisielowski, C.; Yang, L.; Park, C.-H.; Crommie, M. F.; Cohen, M. L.; Louie, S. G.; Zettl, A. *Science* **2009**, *323*, 1705–1708.
(21) Gass, M. H.; Bangert, U.; Bleloch, A. L.; Wang, P.; Nair, R. R.; K., G. *Nature Nanotechnol.* **2008**, *3*, 676–681.
(22) Bhowmick, S.; Waghmare, U. V. *Phys. Rev. B* **2010**, *81*, 155416.
(23) Ding, Y.; Wang, Y.; Ni, J. *Appl. Phys. Lett.* **2009**, *94*, 233107.
(24) Yuge, K. *Phys. Rev. B* **2009**, *79*, 144109.
(25) Giannozzi, P.; et al. *J. Phys.: Condens. Matter* **2009**, *21*, 395502.
(26) Perdew, J. P.; Burke, K.; Ernzerhof, M. *Phys. Rev. Lett.* **1996**, *77*, 3865–3868.
(27) Bengtsson, L. *Phys. Rev. B* **1999**, *59*, 12301–12304.
(28) Nielsen, O. H.; Martin, R. M. *Phys. Rev. B* **1985**, *32*, 3780–3791.
(29) Stone, A. J.; Wales, D. J. *Chem. Phys. Lett.* **1986**, *128*, 501–503.
(30) Bettinger, H. F.; Dumitrică, T.; Scuseria, G. E.; Yakobson, B. I. *Phys. Rev. B* **2002**, *65*, 041406.
(31) Lusk, M. T.; Carr, L. D. *Phys. Rev. Lett.* **2008**, *100*, 175503.
(32) Shenoy, V. B.; Reddy, C. D.; Ramasubramaniam, A.; Zhang, Y. W. *Phys. Rev. Lett.* **2008**, *101*, 245501.
(33) Topsakal, M.; Ciraci, S. *Phys. Rev. B* **2010**, *81*, 024107.
(34) Chen, W.; Li, Y.; Yu, G.; Zhou, Z.; Chen, Z. *J. Chem. Theory Comput.* **2009**, *5*, 3088–3095.
(35) Kokalj, A. *J. Mol. Graphics Model.* **1999**, *17*, 176–179.
(36) Huang, B.; Lee, H.; Gu, B.; Liu, F.; Duan, W. arXiv: 1011.6010v1, 2010.